Properties of an electrochemically deposited Pb monolayer on Cu(111)

Yong S. Chu and Ian K. Robinson
Department of Physics, University of Illinois, Urbana, Illinois 61801

Andrew A. Gewirth
Department of Chemistry, University of Illinois, Urbana, Illinois, 61801

(Received 26 August 1996)

The structure of the electrochemically deposited Pb monolayer on Cu(111) in 0.1*M* $HClO_4$ was studied using *in situ* surface x-ray diffraction. The Pb monolayer forms an unrotated incommensurate hexagonal structure. The nearest-neighbor spacing of the Pb monolayer compresses continuously from 1.4% to 3.2% of the bulk spacing as the electrode potential is varied, with no apparent tendency to lock in. The measured isothermal two-dimensional (2D) compressibility of the Pb monolayer, 0.95 ± 0.07 $Å^2$/eV, is in good agreement with the value expected from the 2D free-electron gas model. The surface normal structure of the Pb monolayer on Cu(111) was studied using reflectivity measurements. Fitting analysis based on a layered model revealed a contracted Pb-Cu spacing and an expanded topmost Cu layer. Unlike the in-plane structure, the surface normal structure showed little potential dependence. [S0163-1829(97)05412-X]

I. INTRODUCTION

As more powerful and sophisticated modern surface science techniques become available, *in situ* measurements of the structure of the electrode-electrolyte interface on an atomic level have become possible. The microscopic structural information available with these techniques can provide better understanding of the atomic-level electrochemical processes that are often strongly influenced by the interface structure. One area of active research is the structure of metal monolayers on the electrode surface deposited through the underpotential deposition (UPD) process. UPD is the electrochemical deposition of foreign metals onto substrates at potentials positive relative to the reversible Nernst potential for bulk deposition.[1] The formation of a stable overlayer before the bulk deposition potential is possible because the adatom-substrate bond is thermodynamically more favorable to the adatom-adatom bond. For this reason, UPD is usually limited to a monolayer in extent, and the resulting structure of the UPD adlayer is strongly influenced by the substrate. The UPD process is an important subject in electrochemistry because of its unique thermodynamic, kinetic, structural, and catalytic properties.[2] In addition to its electrochemical importance, the UPD monolayer is fundamentally significant because it closely resembles an ideal two-dimensional metal under thermodynamic equilibrium conditions. Moreover, since electrochemical conditions are in thermodynamic equilibrium with a reservoir of ions, conditions that are difficult to obtain in the UHV environment, the UPD monolayer is the only practical candidate to study the properties of a two-dimensional metal, within the grand canonical ensemble.

In this work, we examine the structure of Pb UPD monolayer on Cu(111) with *in situ* x-ray diffraction. Although the structures of many UPD systems have been explored previously, most of these works examined only three substrates, gold, silver, and platinum. There are only a small number of reports on the structure of UPD systems on Cu surface.[3,4] The main challenges in performing atomic resolution experiment with copper lie in the difficulties of preparing a clean and smooth surface and keeping it free of oxidation and contaminants for an extended period of time required by data acquisition (several hours for x-ray diffraction). In particular, the requirement on the surface quality is more stringent for spatially averaging probes such as x-ray diffraction than for local probes. Our work demonstrates the feasibility that x-ray diffraction can be used to probe the electrochemical interface of copper.

The Pb UPD process on Cu(111) is known to exhibit a complex and irreversible behavior. The voltammetric features were found to depend strongly on the *p*H of the electrolyte, the prepolarization history, and the types of anions present in the electrolyte.[5,6] Especially, strongly adsorbing anions such as chloride (Cl^-) or acetate (CH_3COOH^-) were reported to affect the kinetics of the UPD process.[6,7] These complicated behaviors generated the hypothesis that the Pb UPD process on Cu(111) might be interfered with by the simultaneous adsorption and/or desorption of either oxygen-containing species such as hydroxide[5,6] (OH^-) or chloride present as a trace impurity in the electrolyte.[7] *In situ* x-ray standing-wave measurements revealed that the layer spacing of the UPD Pb/Cu(111) system changed with the potential. Based on these measurements and some assumptions about the Pb in-plane structure, a model was proposed that oxygen might be incorporated underneath the Pb layer.[4] In this paper, we try to address some of these questions by examining both in-plane and surface normal structures. Also, we investigate the relationship between the kinetic effects with structure, particularly focusing on the effects of chloride on the structure and the properties of the Pb monolayer.

One fundamentally interesting aspect of the Pb monolayer on Cu(111) is that this system is an archetype of large adatoms on a small substrate. In a system of small adatoms on a large substrate atom, the substrate has strong influence on the structure of the adlayer, often resulting in a commensurate adlayer structure. However, the substrate influence is weaker

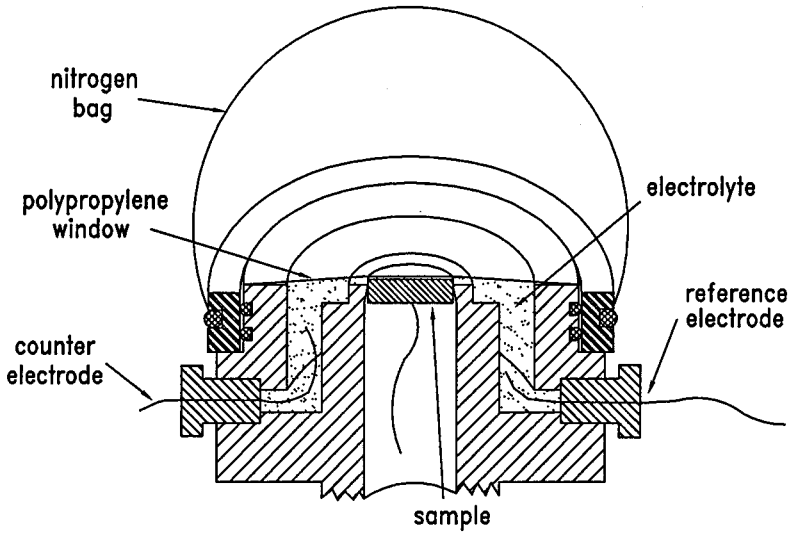

FIG. 1. Schematic drawing of the electrochemical x-ray cell.

for the larger adatoms because the intralayer contacts become important instead, and the resulting structure of the adlayer is often incommensurate. A theoretically interesting case is when the adlayer is rotated with respect to the orientation of the substrate in order to relieve the interfacial strain due to the mismatch of the lattice parameters.[8] In the systems such as Pb/Ag(111),[9] Pb/Au(111),[9] Tl/Ag(111),[9] and Tl/Au(111),[9,10] in which the adatoms are larger than the substrate spacing by about 19–21%, the incommensurate adlayers were found to be rotated by a few degrees. It is interesting to see if a similar rotation exists for Pb/Cu(111) in which the lattice mismatch is even larger (about 37%). There are some differences in the findings for the structure of evaporated Pb films on Cu(111) in vacuum,[11–13] and the differences may be due to the different levels of accuracy in the measurements or nonequilibrium behavior at the interface. Here we examine the structure of Pb/Cu(111) under thermodynamic equilibrium conditions as a function of electrode potential.

For many electrochemically adsorbed layers,[9,10,14,15] the nearest-neighbor spacing changes with the electrode potential. As the electrode potential decreases, the Fermi level for the electrons in the working electrode (sample) increases, leading to the reduction of more metal ions and their incorporation into the UPD layer as neutral atoms. To accommodate a greater number of adatoms on the surface, the lateral spacing of the UPD monolayer must compress. We will closely examine the compression behavior of the Pb monolayer on Cu(111) and compare it with the expected behavior of the corresponding ideal (2D) electron gas.

II. EXPERIMENT

The sample used for experiment was a Cu(111) single crystal (Monocrystal Co.). The sample, 13 mm in diameter and 99.999% in purity, exhibited less than 0.5° miscut. It was mechanically polished using alumina powder down to 0.3 μm and electropolished for 3 min. with a slow stirring in a hanging meniscus geometry with a copper cathode plate. The electropolishing solution was prepared by anodically dissolving Cu into 40% H_3PO_4 at about 100–200 mA/cm^2 for a few hours until the color of the solution turned bright blue. The polishing potential was carefully chosen to be near the end of the anode plateau region, which produced the best polished surface. The typical potential and current density were 1.3 V versus cathodic copper plate and 30–60 mA/cm^2, respectively. After the electropolishing, the sample was rinsed with ample amount of Millipore water (18.2 MΩ cm), quickly blow dried with N_2, and mounted in the Teflon x-ray cell. This method of polishing consistently yielded atomically flat surfaces with a typical mosaic of 0.1°.

The Teflon x-ray cell used for the experiment is shown in Fig. 1. It consists of a tapered center collet for holding the sample, a pocket for electrolyte, an x-ray window, and the side ports for inlet and/or outlet of electrolyte and for electrodes. This cell is similar to the cells used by other x-ray diffraction experiments,[16,17] but it uses a different sample holding method. The sample is inserted from the bottom of the collet and mounted slightly above the cell wall to allow the grazing incident measurements. The sample collet, tapered slightly inward at the end, ensures a tight seal around the crystal. This method of holding the sample reduces the background in the voltammetry by eliminating the unwanted current from the side and the bottom of the sample. A 6-μm polypropylene membrane (Chemplex Inc.) was used as an x-ray window and to contain the electrolyte in the cell. An excellent seal is achieved with a tightly fitted ring around the cell with a thin O ring. To prevent diffusion of oxygen through the thin membrane, N_2 gas was flushed in the outer plastic bag. A gold wire (99.999%, Aldrich) was used for the counter electrode, and a lead wire (99.999%, Aldrich) was used for the reference electrode, in order to make a correct reference to the Pb bulk deposition potential and to prevent a possible anion contamination from commonly used electrodes such as a Ag/AgCl reference electrode. The volume occupied by the electrolyte was about 15 cm^3. The inlet and outlet of the cell were connected to supplying and draining bottles with Teflon tubing and valves (Rainin Co.). The electrolyte consisted with 0.1M $HClO_4$ (Ultrex by J. T. Baker and Millipore water) and 5 mM PbO (99.999%, Aldrich). The electrolyte was deoxygenated with Ar gas (99.998%) in the supplying bottle before filling the cell. After purging the

entire system with Ar gas, the deoxygenated electrolyte was pumped into the cell by pressurizing the supplying bottle with Ar gas. The cell was filled until the membrane expanded to leave a few mm thick electrolyte over the sample. Then, cyclic voltammetry measurements were made to make sure that there were no unusual peaks associated with the presence of impurities. The manipulation of the electrode potential was always done with the expanded membrane (thick-film geometry) to avoid possible complications due to local depletion of Pb ions. Before the x-ray measurements were made, the cell was partially drained, leaving only a thin capillary electrolyte film (thin-film geometry) over the sample. This thin film is crucial to ensure good x-ray penetration to the sample and to help maintain the uniform potential control on the sample surface. A typical procedure for the x-ray diffraction measurements was as follows. The sample was first aligned using the bulk Bragg peaks, and the surface quality of the sample was checked by measuring the bulk crystal truncation rods (CTR) of the substrate, which characterize the surface roughness of the substrate.[18] During the x-ray diffraction measurements, the quality of the surface was frequently checked by monitoring the voltammetric response of the sample (i.e., width of the UPD peak) and the intensity of the CTR peaks. When the surface of the sample became roughened, the experiment was stopped and the sample was repolished.

Surface x-ray diffraction measurements were performed at the National Synchrotron Light Source (NSLS) at beam line X16C. The energy of the beam at 8.5006 keV ($\lambda = 1.45855$ Å) was selected using a Si(111) double-crystal monochromator. The x-ray beam produced from the bending magnet was focused with a Saggital focus monochromator down to a size of about 0.5 mm$\times$2 mm at the focal point and yielded an approximate photon flux of 10^{11} mm^{-2}/s^{-1}. The incident and exit beam of the sample was defined by the vertical parallel slits at 1 mm, and the horizontal exit slit was set at 5 mm. The intensity of the diffracted beam was measured with a NaI scintillation detector. The sample was mounted on a four-circle Kappa diffractometer,[19] custom designed to fit in the small space of the X16C hutch. Throughout this paper, the coordinates of reciprocal space are indexed using a hexagonal coordinate system which is the convention used in low-energy electron diffraction and makes the continuous perpendicular momentum transfer spanned by a single variable. In the hexagonal coordinate system, H and K describe the projection of the wave vector in the plane of the surface, and L alone describes the projection of the wave vector along the surface normal direction. No such simple indexing is possible in the cubic coordinate system. The hexagonal index $(H,K,L)_{\text{hex}}$ is related to the cubic index $(h,k,l)_{\text{cubic}}$ by the transformation

$$\begin{pmatrix} H \\ K \\ L \end{pmatrix} = \begin{pmatrix} -\frac{1}{2} & \frac{1}{2} & 0 \\ 0 & -\frac{1}{2} & \frac{1}{2} \\ 1 & 1 & 1 \end{pmatrix} \begin{pmatrix} h \\ k \\ l \end{pmatrix}. \quad (1)$$

For example, $(0,0,3)_{\text{hex}}=(1,1,1)_{\text{bulk}}$, $(-1,0,2)_{\text{hex}}=(2,0,0)_{\text{bulk}}$, and $(1,0,4)_{\text{hex}}=(0,2,2)_{\text{bulk}}$. The in-plane diffraction measurements were performed at $L=0.2$, corresponding to a grazing incident angle of about 1.3°, in order to avoid the background from the bulk. The measurements at lower L values was not practical because of absorption in the electrolyte at very small grazing angles. Unless otherwise specified, $L=0.2$ is assumed and only (H,K) reciprocal coordinates will be given in the rest of the paper.

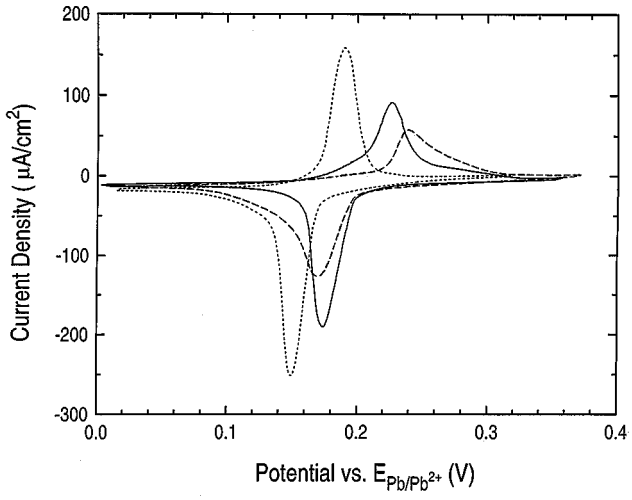

FIG. 2. Voltammetric responses of Pb UPD on Cu(111) under various conditions; 10 min after filling the cell with 0.1M $HClO_4$ + 5 mM PbO (solid line), 11 h after the fill (dashed line), and after 0.4 mM NaCl was added (dotted line). All voltammograms were taken at 10 mV/s.

III. RESULTS

A. Voltammetry

Cyclic voltammetry from the electropolished Cu(111) sample obtained under various conditions are shown in Fig. 2. These voltammograms were measured with a scan rate of 10 mV/s in the x-ray cell prior to the x-ray measurements. The voltammogram plotted with a solid line was obtained 10 min after the cell was filled with the electrolyte consisting of 0.1M $HClO_4$and 5 mM PbO. The voltammogram with a dashed line was taken about 11 h later in the same electrolyte. During these 11 h, the x-ray measurements were performed, requiring extensive cycling of the potential and a number of 30–60-minute-long polarizations with a fully formed Pb monolayer coverage. The dotted voltammogram was taken after introducing a small amount of chloride (0.4 mM NaCl) in the system. In these voltammograms, the current density (μA/cm^2) is plotted against the electrode potential referenced versus the bulk deposition potential of Pb (Nernst potential), which is about -0.460 V versus SCE (saturated calomel electrode) at this Pb concentration. There are two prominent peaks, one in each scan direction. The cathodic (negative current) peak corresponds to deposition of one Pb monolayer on the Cu(111) surface, while the anodic (positive current) peak corresponds to stripping of the deposited Pb monolayer. In all three voltammograms, the deposition and stripping do not occur at the same potential; the stripping always occurs at a higher potential. This potential separation of the deposition peak and stripping peak is due to irreversibility and slow kinetics associated with deposition and/or stripping of the Pb UPD layer, and the size of sepa-

ration increases with the potential scan rate.[6,7] Similar irreversibility was also observed in the Pb UPD process on other substrates.[9] This question of irreversibility will be discussed later in detail.

After 11 h of potential cycling and polarizations, the voltammetric response changed somewhat; the peaks changed their position slightly and their width became much broader. The broadening of the peaks is probably due to roughening of the copper surface, and the change in voltammetric features due to extended polarizations is consistent with the findings of Siegenthaler and Jüttner.[5] Upon addition of 0.4 m*M* chloride in the system, dramatic changes in both the position and the shape of the peaks occurred. The peaks became sharper, the peak current densities increased significantly, and the potential separation between the two peaks became narrower. In addition, both the deposition and stripping peaks were shifted to more negative potentials. Such change in voltammetric response was also reported by Vilche and Jüttner[6] and Brisard *et al.*[7] Although our voltammograms are in good agreement with those of Siegenthaler and Jüttner and Vilche and Jüttner they are not in good agreement with Brisard *et al.* in that our voltammograms obtained in the chloride-free electrolyte are similar to their voltammogram obtained in the electrolyte with a small amount of chloride. Therefore, in spite of all our precautions, it is possible that our chloride-free electrolyte might contain a trace amount of chloride.

B. In-plane structure

Grazing incident angle x-ray diffraction measurements were performed to determine the structure of the underpotentially deposited Pb monolayer on Cu(111) surface. Intense surface diffraction peaks (about 20 000 counts/s) with a small mosaic spread (about 0.5°) indicated a well-ordered Pb overlayer. Throughout the entire UPD potential range, the main diffraction peaks were found at $(x,0)$ and $(0,x)$, where the value for x ranged between 0.741 and 0.754 depending on the electrode potential. Weaker but pronounced higher-order peaks were also found at (x,x), $(2x,0)$, $(2x,2x)$, and $(3x,0)$. Diffraction peaks were found also at all other symmetrically equivalent positions. The pattern of the Pb diffraction peaks is consistent with an incommensurate close-packed hexagonal structure, which is aligned exactly with the Cu(111) substrate. The model of the in-plane structure of the Pb UPD monolayer, probed by grazing incident angle x-ray diffraction measurements, is shown in Fig. 3. This model is in accord with the structure of Pb UPD on Cu(111) determined by *in situ* AFM measurements.[20]

Throughout the entire potential range where the Pb monolayer is stable (i.e., between the bulk deposition potential and stripping potential), the Pb monolayer exhibited only the incommensurate close-packed hexagonal structure. However, the lateral nearest-neighbor spacing showed a significant potential dependence. The in-plane Pb diffraction peaks scanned along the (10) direction (radial direction) and the (12) direction (transverse direction) at different electrode potentials are displayed in Figs. 4(a) and Fig. 4(b), respectively. The position of the diffraction peak scanned along the transverse direction [Fig. 4(a)] remained at $K=0$, as the potential changed from 0.180 to 0.005 V relative to the bulk deposition potential. If the Pb monolayer were rotated with respect to the substrate, there would be two orientational domains, and the transverse scan would have therefore revealed two symmetric peaks separated equally from the origin. Thus, the change in the electrode potential did not affect the alignment

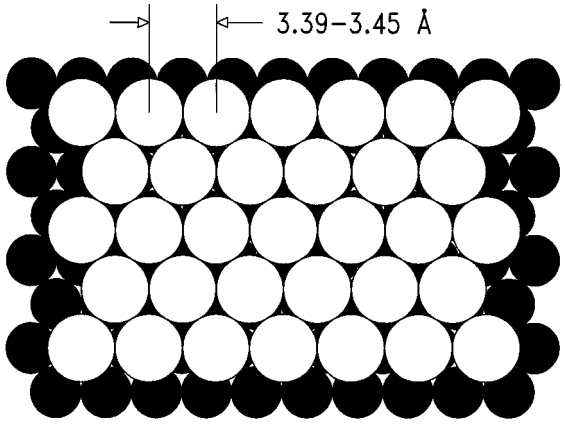

FIG. 3. Proposed model for the structure of Pb UPD monolayer on Cu(111). The small solid circles represent the Cu(111) substrate atoms while the larger open circles represent the Pb adatoms in the unrotated incommensurate hexagonal structure. The spacing of the Pb monolayer varies from about 3.45 to 3.39 Å depending on the electrode potential.

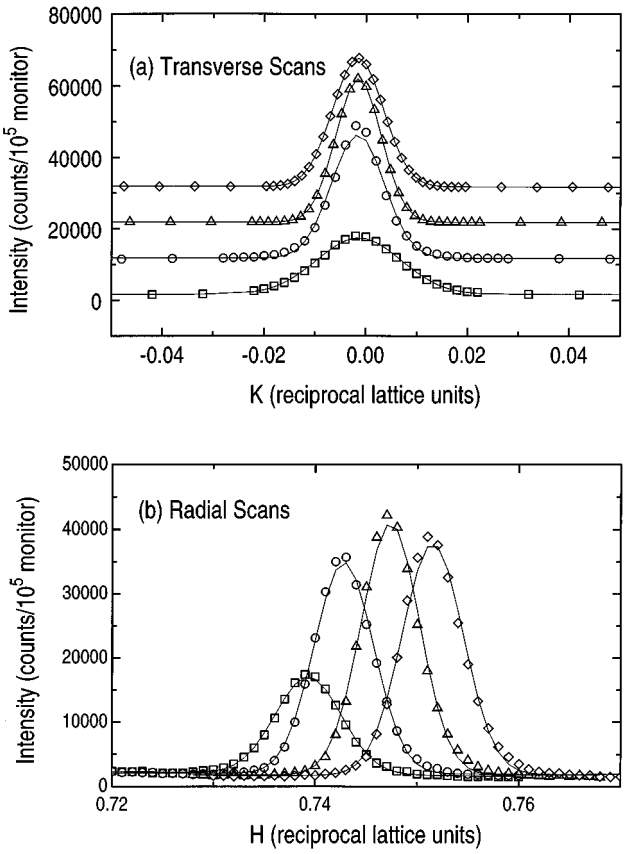

FIG. 4. Profiles of the first-order Pb diffraction peaks at various electrode potentials; transverse (a) and radial (b) scans; 0.180 V (squares), 0.120 V (circles), 0.060 V (triangles), and 0.005 V (diamonds). The transverse scans are shifted vertically for better viewing. The solid lines are the Gaussian fits to the data.

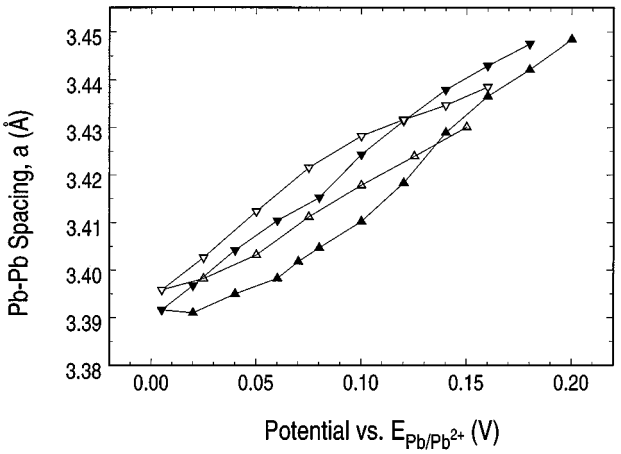

FIG. 5. Compression curves. The nearest-neighbor spacing of Pb monolayer versus the electrode potential; in chloride-free electrolyte (solid triangles) and in chloride-containing (0.4 m*M*) electrolyte (hollow triangles). The data collected while decreasing (increasing) the potential are represented by triangles pointing down (up).

of the Pb monolayer with the substrate. However, narrowing of the transverse peaks suggests that the ordering of the Pb monolayer increased with decreasing potential. Unlike the transverse scans, the radial scans [Fig. 4(b)] do show shifting of peak position with potential. As the potential decreased from 0.180 V to 0.005 V, the radial peak position in H changed from 0.741 to 0.754. The nearest neighbor spacing for the Pb monolayer can be obtained from the radial peak position H, with the relation, $a_{\mathrm{Pb}}=a_{\mathrm{Cu}}/H$, where the nearest-neighbor spacing for Cu(111), a_{Cu}, is 2.556 Å. Therefore, the change in the peak position from 0.741 to 0.754 translates into a change in the nearest-neighbor spacing for the Pb monolayer from 3.448 to 3.392 Å. Consequently, the Pb coverage θ $[=(a_{\mathrm{Cu}}/a_{\mathrm{Pb}})^2=H^2]$ has increased from 0.550 to 0.568 in units of monolayers of Cu(111).

The measured in-plane spacing of the Pb monolayer as a function of the electrode potential is shown in Fig. 5. The data represented by solid triangles were obtained in the chloride-free electrolyte (0.1*M* $HClO_4$+5 m*M* PbO), and the data represented by hollow triangles in the chloride-containing electrolyte (0.1*M* $HClO_4$+5 m*M* PbO + 0.4 m*M* NaCl). Each data point was obtained from the diffraction peak position along the radial direction. As observed for most electrochemically deposited overlayers,[9,10,14,15,21] the nearest-neighbor spacing of Pb UPD monolayer on Cu(111) changes linearly with the electrode potential. One remarkable difference in our case, however, is a large hysteresis; the Pb nearest-neighbor spacing is always smaller during the anodic scan (increasing potential). The hysteresis is probably due to a slow kinetics associated with reaching the electrochemical equilibrium and the formation of an ordered Pb layer as confirmed by the observations: (i) at a fixed potential, the Pb spacing was found to change slowly with time, and (ii) the observed Pb spacing was found to depend also on such factors as the potential scan rate and the electrolyte film thickness. In order to reduce the fluctuation of data due to the hysteresis, a careful procedure was adopted. The initial potential for the measurements was always near the cathodic peak potential. After the potential was set at the desired value, a fixed interval of time was allowed to pass before the membrane was deflated to the thin-film geometry for x-ray measurements, and an almost equal amount of time was used to collect data at each potential. After the measurements, the membrane was restored to the thick- film geometry, and the potential was scanned down to the next desired value at a rate of 1 mV/s. This procedure was repeated until the potential reached 5 mV above the Pb bulk deposition potential. Then, the direction of potential scan was reversed, and the same procedure was repeated. The data shown in Fig. 5 were obtained with a 3-min waiting interval before deflating the membrane. Although a lower scan rate and a longer waiting interval decreased the magnitude of the hysteresis, it still persisted even when a 0.1-mV/s scan rate and a 30-min waiting interval were employed. The scan rate of 1 mV/s and waiting interval of 3 min were chosen because the complete set of data had to be measured before the sample surface became noticeably roughened, usually after 15–20 h. In addition to the hysteresis in the position of the diffraction peaks, the intensities and widths also show a weak dependence on the potential scan direction. The diffraction peaks measured during the anodic scan (increasing potential) were slightly but consistently stronger and narrower than the peaks measured during the cathodic scan (decreasing potential), indicating that the Pb-monolayer-obtained increasing potential is more ordered than the decreasing potential. The observed hysteresis, arising from a large equilibrium time constant for the formation of the ordered overlayer, suggests that there exists an activation energy associated with adding and taking away a Pb adatom. A similar hysteresis was also observed for the diffraction profiles of the electrochemically adsorbed iodine monolayer on Au(111).[21] The hysteresis observed in the diffraction peaks should be distinguished from the irreversibility seen in the voltammetry, in which the deposition and stripping of the UPD monolayer do not occur at the same potential (see Fig. 2). The voltammetric irreversibility only reflects the hysteresis associated with the charge transfer needed for formation and stripping of the Pb UPD monolayer. The time constant for the charge transfer is on the order of several seconds and can be measured by a potential step method or estimated from the width of the voltammetric peaks. On the other hand, the potential dependence of the diffraction peaks measures the hysteresis associated with adding (removing) additional adatoms into (out of) an ordered Pb overlayer, and the subsequent relaxation of the layer. The time constant for the structural response to the potential is much larger (on the order of several minutes).

The compression data shown in Fig. 5 can be used to calculate the two-dimensional isothermal compressibility of the Pb UPD monolayer. The isothermal compressibility, $\kappa_{2\mathrm{D}}$, for the electrochemically deposited layer with a hexagonal structure is given by[9,22]

$$\kappa_{2\mathrm{D}}=\frac{\sqrt{3}a}{ne}\left(\frac{\partial a}{\partial V}\right)_T, \tag{2}$$

where n is the number of electrons required for oxidation or reduction of the adatom (i.e., $\mathrm{Pb}=\mathrm{Pb}^{n+}+ne^-$, $n=2$), and V is the electrode potential. The quantity $(\partial a/\partial V)_T$ is the measured slope of the electrocompression data. Although the

large hysteresis presented in our data makes estimation of the slope difficult, the data were reasonably represented when fitted with a line going through the middle of the hysteresis loop. The two-dimensional isothermal compressibility of Pb on Cu(111), estimated with the linear fit of data, was 0.95 ± 0.07 Å^2/eV. This value is smaller than the previously measured values for the Pb UPD monolayer on Ag(111) and Au(111), 1.25 ± 0.05 Å^2/eV and 1.69 ± 0.10 Å^2/eV, respectively.[9]

In order to study the anion effects on the UPD Pb monolayer, a small known amount of chloride (0.4 m*M*) was introduced to the system. The packing arrangement of the Pb monolayer on Cu(111) was not affected by the presence of chloride. The Pb monolayer still formed an unrotated hexagonal close-packed structure. However, the presence of chloride in the electrolyte influenced the compression behavior of the Pb monolayer. The data represented by hollow triangles in Fig. 5 are the compression curve of the Pb monolayer obtained in an chloride containing electrolyte (0.1*M* $HClO_4$+5 m*M* PbO+0.4 m*M* NaCl) and otherwise under identical condition. The effects of chloride on the compression behavior of the Pb monolayer are clearly seen. One of the most apparent effects is the increase in the Pb-Pb spacing, especially in the lower UPD potential region (<0.12 V). Another way to appreciate this apparent increase in the Pb-Pb spacing is in terms of a shift in the compression curve. A large portion of both compression curves overlap if the compression curve obtained in the chloride-containing electrolyte is shifted by about 25 mV. This shift of the compression curve is consistent with the voltammetric response of the system, in which the deposition peak of the Pb monolayer is typically shifted to more negative potentials upon addition of specifically adsorbing anions such as chloride and acetate, and the amount of shift depends on the concentration and the type of anions[6,7]. In our case, a shift of -25 mV was observed at 0.4 m*M* chloride concentration as shown in Fig. 2. This shift in the voltammetry is not just kinetic effects but an actual change in the deposition potential. For example, the Pb diffraction peak was never observed at 0.18 V upon decreasing the potential in the electrolyte with 0.4 m*M* chloride. Consequently, the compression of the Pb monolayer is expected to be lagged in potential, because the rates of compression in both electrolytes are comparable. In addition, the presence of chloride in the electrolyte decreased the compression hysteresis. This is consistent with the voltammetric response of the system (see Fig. 2) and an interpretation that the UPD process becomes more reversible and enhanced in its kinetics with addition of chloride.[6,7] Another effect of chloride is a decrease in the slope of the compression curve. Since the 2D compressibility is obtained from the slope of the compression curve, the decrease in the slope indicates a decrease in the compressibility of the Pb monolayer. The measured compressibility in the chloride-containing electrolyte is 0.79 ± 0.09 Å^2/eV. This is a 17% $\pm 11\%$ change. In addition to the effects exhibited in Fig. 5, the influence of chloride was also manifested in the profiles of the Pb diffraction peak. After adding chloride, the diffraction peak became noticeably weaker and wider, indicating that the Pb monolayer was less well ordered with chloride. The change in the compressibility and the broadening of the diffraction suggests that the effect of chloride on the structure of the Pb monolayer and its compression property is not negligible. The compression curve measured at 4 m*M* chloride concentration (data not shown) exhibited much greater chloride effects. However, these measurements may have been hampered by white precipitants visible on the surface (probably $PbCl_2$), which significantly changed the voltammetry and severely weakened the Pb diffraction peaks.

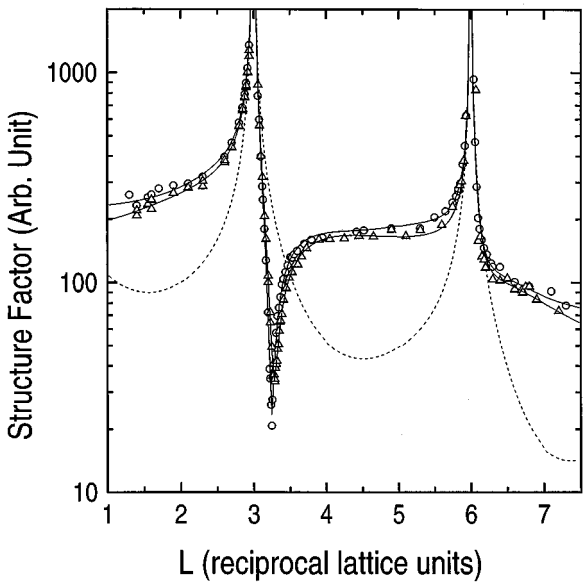

FIG. 6. Reflectivity data at 0.160 V (triangles) and at 0.050 V (circles). The lines are the best fits to the data using Eq. (3). The calculation for a perfectly terminated Cu(111) surface without Pb is represented by the dashed line.

C. Surface normal structure

The surface normal structure of the underpotentially deposited Pb monolayer was probed using the x-ray reflectivity measurement. Reflectivity is a well-established technique to measure the electron density profile in the surface normal direction.[23] Figure 6 shows the reflectivity measurements at two different potentials, 0.160 and 0.050 V in the chloride-free electrolyte. The data are represented by the hollow symbols and the solid curves are the best fits to the data. The dashed curve is the calculated reflectivity curve of the ideally terminated bare Cu(111) surface. Each data point was obtained by integrating the ω rocking curves at each L value in order to remove the background due mainly to scattering from the solution and membrane. The divergent behavior at $L=3$ and 6 is due to $(0,0,3)_{\text{hex}}$ or $(1,1,1)_{\text{cubic}}$ and $(0,0,6)_{\text{hex}}$ or $(2,2,2)_{\text{cubic}}$ bulk Bragg peaks. Both data sets deviate significantly from the calculated curve for the ideally terminated surface. The dramatic modulations around the Bragg peaks are due to the constructive and destructive interference between the amplitudes scattered by the substrate and the much heavier Pb monolayer on the surface. Although the data measured at both potentials look very similar, a careful inspection reveals some fine differences. The data taken at 0.05 V are slightly larger on the shoulders to the left of the Bragg peaks and smaller at the minimum. Also, the minimum at 0.05 V is slightly narrower and is located slightly closer to the Bragg peak. These difference are consistent

TABLE I. Fit results of the reflectivity data.

E (V)	Atom	Spacing (Å)	σ (Å)	Coverage
0.160	Cu	2.096 ± 0.009	0.09 ± 0.03	1 (fixed)
	Pb	2.519 ± 0.011	0.21 ± 0.01	0.52 ± 0.02
0.050	Cu	2.111 ± 0.009	0.09 ± 0.02	1 (fixed)
	Pb	2.497 ± 0.011	0.21 ± 0.01	0.58 ± 0.02

with the increase in Pb coverage. The detail of the surface normal structure is obtained by fitting the data with a layered model. Since the density of the water is much smaller than the density of Pb, the data were easily fitted with a simple model including only a monolayer of Pb and bulk Cu(111) substrate with a relaxed top layer. The reflected intensity is given by the square of the structure factor, which is written as

$$|F(q_z)|^2 = e^{q_{\rm abs}/q_z}\Big| f_{\rm Cu}(q_z)e^{-q_z^2\sigma_{\rm B}^2/2}\sum_{n=0}^{n=\infty} e^{-ind_{\rm B}q_z} + f_{\rm Cu}(q_z)e^{-q_z^2\sigma_{\rm Cu}^2/2}e^{id_{\rm Cu}q_z} + \theta_{\rm Pb}f_{\rm Pb}(q_z)e^{-q_z^2\sigma_{\rm Pb}^2/2}e^{id_{\rm Pb}q_z}\Big|^2 . \quad (3)$$

The first term is the contribution from the bulk Cu(111) where the summation over n represents the semi-infinite crystal. The second and the third terms represent the contributions from the topmost Cu layer and the deposited Pb monolayer, respectively. The parameters pertaining to the bulk, the topmost Cu layer, and the Pb layer are denoted with labels B, Cu, and Pb. The quantity $f(q_z)$ is the atomic scattering form factor, which approaches the number of electrons in the atom as q_z becomes small. The Debye-Waller factor $e^{-q_z^2\sigma^2/2}$ accounts for thermal vibration of the atoms as a root-mean-square (rms) atomic displacement σ. The parameter d is the position of the layer in question. The parameter $\theta_{\rm Pb}$ is the coverage of the Pb layer, and the coverage of the topmost Cu layer is assumed to be unity. The prefactor $e^{q_{\rm abs}/q_z}$ is the correction factor for the absorption by the thin electrolyte film over the surface, and $q_{\rm abs}=0.10$ Å^{-1} was obtained from the fits. In the fitting analysis, the bulk spacing $d_{\rm B}$ and Debye-Waller parameter $\sigma_{\rm B}$ were fixed at their bulk values, 2.087 and 0.085 Å,[29] respectively, but all other parameters were allowed to vary. The proposed model produced excellent fits for both data sets ($\chi^2=1.17$ for data at 0.160 V and $\chi^2=0.67$ for 0.050 V). The fit parameter results are listed in Table I.

At 0.160 V, the coverage of the Pb monolayer, 0.52 ± 0.02, is close to the coverage of 0.55 based on the Pb lateral spacing. The spacing of the topmost Cu layer, 2.096 ± 0.009 Å, is slightly (0.5%) expanded from the bulk spacing. The Debye-Waller parameter for the topmost Cu atoms, 0.09 ± 0.03 Å, and the deposited Pb atoms, 0.21 ± 0.01 Å, are in a good agreement with the bulk values, 0.085 and 0.206 Å, respectively. The spacing between the Pb monolayer and the topmost Cu layer ($d_{\rm Pb}$-$d_{\rm Cu}$) turned out to be 2.519 ± 0.011 Å. The average bond length of Pb-Cu can be calculated under the assumption that there is no preferred site for Pb atoms and all possible relative positions of Pb atom with respect to the nearest Cu atom are equally probable, which is a valid assumption for an ideally incommensurate structure. The calculated average bond length is 2.68 ± 0.05 Å, while the bond length for top site, bridge site, and hollow site would be 2.52, 2.82, and 2.92 Å, respectively. The average bond length is significantly smaller than 3.03 Å, the average of the radii for bulk Pb (3.50 Å) and Cu (2.56 Å), suggesting a considerable bonding between Pb and Cu. The only significant change in the surface normal structure with the potential was the Pb coverage. At 0.05 V, the Pb coverage obtained from the fits is 0.58, which is in good agreement with 0.57, the estimated coverage based on the in-plane Pb spacing. The change in all other parameters are well within the errors.

Other models were also used to fit the data to investigate the possibility of different structures. An additional layer of Pb was added with a variable coverage, but that value refined to zero, giving convincing evidence that the underpotential deposition of Pb on Cu(111) is limited only to a single monolayer. The voltammetric peaks become significantly wider after extensive potential cycling and/or long polarizations with a full coverage of the Pb monolayer, which raises the question of the possibility of surface alloying. To test this possibility, the data were fitted using various models allowing the presence of Pb below the Cu surface. These models all failed to fit the data, giving large χ^2 and moreover produced unphysical parameter values. Therefore, the formation of surface alloying during the time required for the measurements (about 10 h) is undetectable.

IV. DISCUSSION

Our *in situ* surface x-ray diffraction study demonstrated that UPD Pb on Cu(111) forms an ordered incommensurate close-packed hexagonal monolayer structure, exactly aligned with the substrate. Although the packing arrangement and alignment of the Pb monolayer with the substrate did not show any potential dependence, the spacing continuously changed from 3.448 to 3.392 Å. No locking in of the Pb spacing was observed at a possible commensurate (4×4) structure that corresponds to the Pb spacing of 3.408 Å, in the middle of this range. Thus, the Pb monolayer behaved much like a two-dimensional floating layer unaffected by the periodic potential of the substrate. In the past, there have been four reports on the structure of Pb monolayer on Cu(111): three on the evaporated Pb film in vacuum[11–13] and one on the Pb UPD monolayer emersed into vacuum.[7] The first two of these studies claimed a commensurate $p(4\times4)$ structure, whereas the later two claimed an incommensurate hexagonal structure. It is possible that the older measurements lacked the accuracy to distinguish between the $p(4\times4)$ and incommensurate structures. In addition, Refs. 11 and 12 reported an abrupt change in the lattice parameter with the coverage, while Ref. 13 observed a more gradual change. These findings are qualitatively consistent with our results. The sudden change of the lattice parameter of the Pb layer may be due to nonequilibrium behavior at the interface during the vapor deposition. One interesting finding of Ref. 7 is that the spacing of the Pb monolayer was the same as the

bulk value, regardless of the emersion potential. This suggests that the compressed Pb spacing may have become relaxed to its natural spacing after the loss of potential control. Despite some quantitative differences, the structure of evaporated Pb film on Cu(111) and the underpotentially deposited Pb monolayer on Cu(111) are apparently the same.

While the electrochemically deposited and evaporated Pb monolayers on Cu(111) share a common structure, the Pb monolayer exhibits different structures on different substrates, in particular Au(111) and Ag(111). Although the Pb monolayer forms an incommensurate hexagonal structure on all three substrates, it has different rotation angles with respect to the substrate orientation. On a Ag(111) substrate prepared by evaporating Ag film on mica, the Pb monolayer was rotated with a fixed rotation angle of 4.5°.[9] On the evaporated Au(111) film on mica, the rotation angle showed a potential dependence: 2.5° for the potential less than 0.13 V and 0° for the potential larger than 0.16 V.[9] In contrast, for the Pb monolayer on the Au(111) single crystal, the rotation angle changed continuously from about 2° at 0.21 V to 3.7° at 0.05 V with a large hysteresis.[25] The discrepancy between the Au(111) film and the single-crystal results may be due to a very large mosaic present in the evaporated Au(111) film. According the theory of McTague and Novaco,[8] an epitaxial overlayer should rotate with respect to the substrate to reduce the strain energy due the mismatch of the lattice parameters, and the rotation should increase with the increasing mismatch. The theory predicts a rotation angle of 5–6° on both Ag(111) and Au(111) (about 21% mismatch) and 8–9° on Cu(111) (about 37% mismatch). Moreover, the rotation angle should decrease as the potential decreases because the decreasing potential compresses the spacing of the Pb layer, reducing the misfit. Although the theory seems to be in qualitative agreement regarding the rotation of the Pb monolayer on Au(111) and Ag(111), it fails completely in the case of the Pb monolayer on Cu(111), which we find is not rotated at all. In addition, the direction of the potential dependence of the rotation of Pb monolayer on Au(111) is inconsistent with the theory. Considering all the experimental facts, the theory of McTague and Novaco[8] does not work well for the epitaxial metal layer. The reason for the failure may be that the theory is based on phonon interactions between the overlayer and substrate, whereas the electronic effects are more important for a metal overlayer on metal substrate. The absence of rotation in Pb/Cu(111) suggests that the spatial corrugation of the underlying Cu(111) substrate is too fine to impose significant influence on the structure of the much larger adatoms. Despite its quantitative failure in these systems, the theory can still offer some insights. If the rotation is needed to lower the interaction energy between the epitaxial layer and the substrate, the fact that the rotation exists means the substrate influence is not negligible. The absence of rotation in Pb/Cu(111) suggests that the spatial corrugation of the underlying Cu(111) substrate is too fine to impose significant influence on the structure of the much larger adatoms, and the adatom-substrate interaction for Pb/Cu(111) is expected to be smaller than for Pb/Ag(111) and Pb/Au(111).

Although it is plausible to think that the lack of rotation in the Pb/Cu(111) system is attributed to the large size difference between Pb and Cu atoms, a possibility exists that the lack of rotation may be extrinsic, due to defects or impurities on the substrate as observed in some systems of physisorbed noble gases. For example, for Xe/Ag(111), the lack of a 30 ° rotation predicted by the theory of McTague and Novaco[8,26] is attributed to the preferential nucleation of the Xe monolayer along the (111) steps.[27] For Kr/Pt(111), rotation angles of 30°, 0°, or both (in coexistence) were observed depending the levels and types impurities blocking the step sites.[28] If there were effects due to steps or impurities, we would expect inhomogeneous distributions of rotation angles as a function of miscut, polishing conditions, and contaminants (Cl^-). In our experiment, four different substrates were used, with different miscut directions (all less than 0.5°). A total of about 20 separate measurements with different levels of chloride concentrations were performed on these substrates, each time freshly repolished, but we never observed a rotated Pb overlayer. So, we conclude that the lack of rotation was not due to the effects of steps or impurities. However, no matter what the actual reason for the lack of rotation may be, our findings on the compression properties of the Pb monolayer are unaffected.

The compression behavior of the Pb monolayer on Cu(111) can be satisfactorily modeled by the free-electron gas model.[29] The justification for using the free-electron description is that the Pb monolayer does show evidence of a floating 2D layer. In the free-electron gas model of a metal, the 2D compressibility, κ_{2D}, for a closed-packed hexagonal 2D metal is given by[9,30]

$$\kappa_{2D}=\frac{3ma^4}{4\pi\hbar^2Z^2}, \tag{4}$$

where m is the electron mass, a is the nearest-neighbor spacing of the 2D metal, and Z is the number of valence electrons per metal atom. The κ_{2D} computed using $a=3.386$ Å, which is the extrapolated nearest-neighbor spacing at $V=0$ and $Z=4$ is 0.258 $Å^2$/eV, whereas the measured κ_{2D} value using Eq. (2) is 0.95 ± 0.07 $Å^2$/eV. This apparent discrepancy arises because Eq. (2) is derived from general thermodynamic assumptions while Eq. (4) is specific to the free-electron gas model. In order to compare the two values on the same footing, the measured κ_{2D} value must be divided by $Z=4$. After this correction, the experimental κ_{2D} value agrees excellently with the theoretical value based on the free-electron gas model as shown in Fig. 7. In Fig. 7, the data collected during each potential scan direction are fitted separately with a line of fixed slope given by theoretical compressibility in the free-electron gas model. The agreement between the theoretical compressibility value and the measured compressibility values for Pb/Au(111), 1.69 ± 0.1 $Å^2$/eV, and for Pb/Ag(111), 1.25 ± 0.05 $Å^2$/eV, is not very good. The different levels of agreement for these three similar systems are attributed to the difference in the degrees of the interaction between the Pb overlayer and the substrate, which must be added to the free-electron description.[30]

It is interesting to observe that the surface normal structure of the Pb monolayer exhibited little potential dependence while the in-plane spacing was strongly affected by the electrode potential; as the potential changed from 0.160 to 0.050 V, the Pb-Cu bond length remained virtually con-

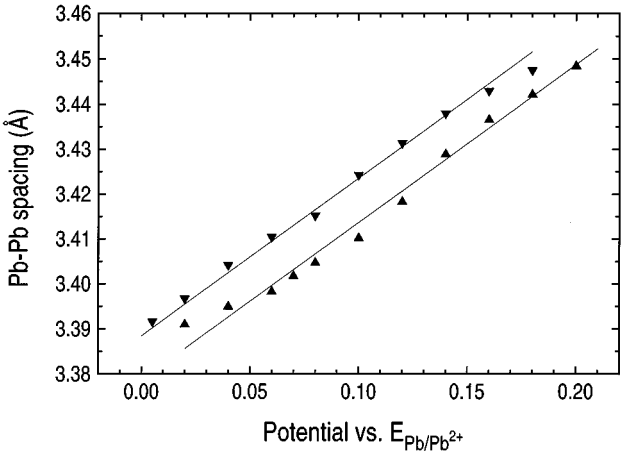

FIG. 7. Comparison between the data and the theoretical compressibility in the free electron gas model. The data obtained in each potential scan direction are fitted separately with a line of fixed slope given by the theoretical compressibility value; downward triangles (decreasing potential); upward triangles (increasing potential).

stant. It implies that the electronic density of the Pb monolayer along the surface normal direction is unaffected by the compression in the plane. This is in complete contrast with the usual three-dimensional situation in which a structure under lateral pressure is vertically expanded.[31] At both potentials, the average Pb-Cu bond length was smaller than the sum of the two metallic radii, and the topmost Cu layer spacing was slightly expanded. This surface normal structure is consistent with that for most metals. The top surface layer spacing of a metal is usually contracted from its bulk spacing in order to lower the energy of the surface layer by increasing effective coordination of the surface atoms, and the second layer is expanded to relieve the strain caused by the contraction of the first layer and to restore the average atomic volume at the surface.[32] In the case of the Pb UPD layer, the Pb monolayer is fully discharged and becomes part of a combined metal-substrate system. Since the Pb layer is the top layer for this combined system, the Pb-Cu spacing is contracted from the ''bulk'' spacing, meaning the sum of the two metallic radii. The topmost Cu layer, now being the second layer of the combined system, is consequently expanded. A similar finding is reported for the underpotentially deposited Tl layer on Au(111).[10]

Our findings on the surface normal structure are in contrast to results of the standing wave measurements by Zegenhagen *et al.*, in which the Pb-Cu spacing depended on the electrode potential.[4] According to their measurements, the Pb-Cu spacing was 2.32 ± 0.07 Å at the potential near the UPD deposition peak and 2.54 ± 0.03 Å near the bulk deposition potential for Pb. Their Pb-Cu spacing near the bulk deposition potential for Pb is in agreement with our results, but the value near the UPD deposition peak is significantly different from ours. In order to explain the unusually small Pb-Cu spacing, they proposed a model in which an oxygen is embedded in the interstitial sites between the first and second Cu layers, and the Pb atom is located at the threefold hollow sites. The interstitial oxygen would cause a outward displacement of three Cu atoms in the first layer, allowing the Pb atom to move downward further. This model is based on incorrect assumptions about the registry of Pb atoms and the Pb coverage. Since the outward displacement is not possible for all the three-fold hollow sites for Cu, in order to accommodate such geometry, the Pb coverage must be much less than 0.52–58, the value confirmed by our in-plane diffraction and reflectivity measurements as well as the previous electrochemical studies.[5–7] The voltammetry of Zegenhagen *et al.* indicates that there is a significant level of oxidation and reduction of the working electrode, which was never observed by others. Therefore, it is possible that the structure for Pb/Cu(111) may be completely different when the copper substrate is significantly oxidized. One way to confirm the results of Zegenhagen *et al.*[4] would be to repeat our experiment in an electrolyte with a higher *p*H.

Since the effects of anions on the Pb UPD process on Cu(111) are of significant interest, the effects of chloride on the UPD Pb/Cu(111) structure deserve more discussion. Anions are known to incorporate into the UPD structures if the UPD layers form open structures.[33] However, it is generally accepted that anions are not involved in a UPD structure if the UPD layer forms a closed structure like the close-packed hexagonal structure.[14,9] We also come to the same conclusion for UPD Pb/Cu(111) in that the packing arrangement of the Pb on Cu(111) is also hexagonal in the chloride-containing electrolyte. However, it is not certain if the specifically adsorbed anions affect the detail of the structure and/or properties. The good agreement between the Pb coverage based on the reflectivity measurements and the estimated values from the in-plane lattice spacing indicates that the chloride is not present inside the Pb monolayer but rather specifically adsorbed on top of the Pb monolayer. This conclusion is supported by the coulometry measurements by Brisard *et al.*[7] Thus, we believe that the change in the compression behavior of the Pb monolayer shown in Fig. 5 is due to the influence of the specifically adsorbed chloride onto the Pb UPD layer. It is probable that the specifically adsorbed chloride affects the valence electron density of the Pb monolayer, modifying the compression behavior of the Pb layer. Though it was not as dramatic, a similar phenomenon was observed by Toney *et al.*[9] At the same electrode potential, they found that the Pb-Pb spacing was slightly larger in the acetate than in the perchlorate. Also, the slope of the compression curve was slightly smaller in the acetate. These findings are in qualitative agreement with our results. A possible reason for the smaller anion effects seen by Toney *et al.* may be that acetate is not as strongly adsorbing an anion as chloride.

V. CONCLUSION

In our experiment, the structure of the Pb UPD monolayer on Cu(111) was studied by surface x-ray diffraction. The Pb UPD monolayer exhibited an unrotated incommensurate hexagonal structure. No other structure was observed throughout the entire UPD potential range. The structure found for the Pb UPD monolayer is consistent with the vapor-deposited Pb monolayer on Cu(111). However, it is different from the structure of Pb UPD monolayer on Au(111) and Ag(111) in which the overlayer was rotated with respect to the substrate.

The in-plane nearest-neighbor spacing of the Pb mono-

layer was found compressed by 1.4–3.2% compared with the Pb bulk spacing. The compression of the Pb monolayer exhibited hysteresis, which is attributed to the slow kinetics and the irreversibility associated with the formation of the ordered Pb layer on Cu(111). Despite the hysteresis, the Pb monolayer on Cu(111) behaved much like an ideal 2D floating layer, exhibiting excellent agreement with the free-electron gas model.[30]

The surface normal structure, probed with the reflectivity measurements, was modeled satisfactorily with a single Pb layer on the relaxed Cu(111) substrate. The coverage obtained from the fits agree well with the estimates based on the in-plane lattice spacing. Unlike the in-plane structure, the surface normal structure showed little potential dependence. Based on the fitting analysis using various models, the possibilities for the deposition of more than one Pb monolayer during the UPD process on Cu(111), or the formation of surface alloy, is negligible.

The presence of chloride in the electrolyte significantly influenced the Pb UPD process. Addition of chloride in the electrolyte enhanced the kinetics and reduced the irreversibility of the UPD process. These effects were manifested through reduction of the hysteresis in the compression behavior of the Pb monolayer. Moreover, a decrease in the compressibility of the Pb monolayer was observed. The influence on the compressibility suggests that the valence electronic density of the Pb monolayer may be affected by the specifically adsorbed chloride.

ACKNOWLEDGMENTS

We thank Ben Ocko for useful discussion and sharing his unpublished data on Pb/Au(111). This work was supported by the U.S. Department of Energy under Contract No. DEFG02-96ER45439. The National Synchrotron Light Source is supported by Department of Energy, Contract No. DEAC012-76CH00016.

[1] D. M. Kolb, *Advances in Electrochemistry and Electrochemical Engineering, Vol. 11*, edited by H. Gerischer and C. W. Tobias (Wiley-Interscience, New York, 1978).
[2] R. Adzic, *Advances in Electrochemistry and Electrochemical Engineering, Vol. 13*, edited by H. Gerischer and C. W. Tobias (Wiley-Interscience, New York, 1978).
[3] M. Ge and A. A. Gewirth, Surf. Sci. **324**, 140 (1995).
[4] J. Zegenhagen, G. Materlik, J. P. Dirks, and M. Schmäh, *Synchrotron Techniques in Interfacial Electrochemistry*, edited by C. A. Melendres and A. Tadjeddine (Kluwer Academic Publishers, Boston, 1994).
[5] H. Siegenthaler and K. Jüttner, Electroanal. Chem. **163**, 327 (1984).
[6] J. R. Vilche and K. Jüttner, Electrochim. Acta. **32**, 1567 (1987).
[7] G. M. Brisard, E. Zentani, H. A. Gasteiger, N. M. Markovíc, and P. N. Ross, Jr., Langmuir, **11**, 2221 (1995).
[8] J. P. McTague and A. D. Novaco, Phys. Rev. B **19**, 5299 (1979).
[9] M. F. Toney, J. G. Gordon, M. G. Samant, G. L. Borges, and O. R. Melroy, J. Phys. Chem. **99**, 4733 (1995).
[10] J. Wang, R. Adzic, and B. Ocko, J. Phys. Chem. **98**, 7182 (1994).
[11] J. Henrion and G. E. Rhead, Surf. Sci. **29**, 20 (1972).
[12] K. J. Rawlings, M. J. Gibson, and P. J. Dobson, J. Phys. D **11**, 2059 (1978).
[13] G. Meyer, M. Michailov, and M. Henzler, Surf. Sci. **189/190**, 1091 (1987).
[14] M. F. Toney, J. G. Gordon, M. G. Samant, G. L. Borges, D. Wiesler, D. Yee, and L. B. Sorensen, Langmuir **7**, 796 (1991).
[15] C.-H. Chen, K. D. Kepler, A. A. Gewirth, B. M. Ocko, and J. Wang, J. Phys. Chem. **97**, 7290 (1993).
[16] M. Samant, M. Toney, G. Borges, L. Blum, and O. Melroy, J. Phys. Chem. **92**, 220 (1988).
[17] B. M. Ocko, J. Wang, A. Davenport, and H. Isaacs, Phys. Rev. Lett. **65**, 1466 (1990).
[18] I. K. Robinson, Phys. Rev. B **33**, 3830 (1986).
[19] I. K. Robinson, H. Graafsma, A. Kvick, and J. Linderholm, Rev. Sci. Instru. **66**, 1765 (1995).
[20] D. D. Sneddon, Ph.D. thesis, University of Illinois, 1995.
[21] B. M. Ocko, G. M. Watson, and Jia Wang, J. Phys. Chem. **94**, 897 (1994).
[22] O. R. Melroy, M. F. Toney, G. L. Borges, M. G. Samant, J. B. Kortright, P. N. Ross, and L. Blum, Phys. Rev. B **38**, 101 962 (1988).
[23] J. Als-Nielsen, *Handbook on Synchrotron Radiation, Vol. III*, edited by G. S. Brown and D. E. Moncton (North-Holland, Amsterdam, 1991).
[24] *International Tables for X-ray Crystallography, Vol. III* (The Kynoch Press, Birmingham, England, 1962).
[25] B. M. Ocko (private communication).
[26] L. W. Bruch and J. M. Phillips, Surf. Sci. **91**, 1 (1980).
[27] P. I. Cohen, J. Unguris, and M. B. Webb, Surf. Sci. **58**, 429 (1796).
[28] K. Kern, P. Zeppenfeld, R. David, R. L. Palmer, and G. Comsa, Phys. Rev. Lett. **57**, 3187 (1986).
[29] N. Ashcroft and N. D. Mermin, *Solid State Physics* (Saunders, Philadelphia, 1976).
[30] Y. S. Chu, Ph.D. thesis, University of Illinois, 1997.
[31] J. P. Hirth and J. Lothe, *Theory Of Dislocations* (Wiley-Interscience, New York, 1982).
[32] A. Zangwill, *Physics at Surfaces* (Cambridge University Press, Cambridge, 1988).
[33] M. F. Toney, J. N. Howard, J. Richer, G. L. Borges, J. G. Gordon, O. R. Melroy, D. Yee, and L. B. Sorensen, Phys. Rev. Lett. **75**, 4472 (1995).